Influence of plastic shear strain on the magnetic behaviour of pure iron

Z. Maazaz, Olivier de La Barrière, Olivier Hubert

Influence of plastic shear strain on the magnetic behaviour of pure iron

Z. Maazaz[a], O. de la Barrière[b], O. Hubert[a]

[a] *Université Paris-Saclay, CentraleSupélec, ENS Paris-Saclay, CNRS, LMPS - Laboratoire de Mécanique Paris-Saclay, 91190, Gif-sur-Yvette, France*
[b] *Université Paris-Saclay, ENS Paris-Saclay, CNRS, SATIE Paris-Saclay, 91190, Gif-sur-Yvette, France*

Abstract

The effect of plastic strain on magnetic behaviour was studied earlier by many authors. These studies mainly focused on plastic straining obtained by tensile testing and on magnetic measurement along the tensile axis. We present in this paper some new results showing the influence of a plastic shear strain obtained thanks to a torsion test on the magnetic behaviour of a pure iron. These results highlight the dominant role of the cumulative plastic strain on the magnetic behaviour.

Keywords: Pure iron, plastic shear strain, magnetic hysteresis, magneto-plastic modeling

1. Introduction

The study and modeling of the effects of the mechanical state on the magnetic properties of materials remains an ongoing challenge [1, 2]. A better understanding and modeling of the effect of plasticity (permanent deformation) is particularly sought. Applications are numerous: improving the predictivity of electromagnetic non-destructive testing [3]; better control the influence of cutting on the performance of electrical steels [4]. Previous research has mainly focused on the influence of tensile plastic deformation on magnetic behavior [5, 6, 7, 8] or magnetic domains structure [9] thus leading to different interpretations. In this work, plasticity is obtained through a torsion test. We then study the influence of this plastic shear strain on the magnetic behavior of pure iron. Results are discussed in terms of the influence of defects and residual stresses.

2. Protocol

The material employed in this investigation is a pure iron (ARMCO grade). This material exhibits a single ferrite untexturized phase as illustrated in figure 1. The torsion test is probably the most suitable test for carrying out plastic shear deformation. It consists of applying a torque $\vec{C}$ along the z axis of a tubular test piece (figure 2a). The torque produces a twist angle α. Under these conditions stress and deformation tensors $\boldsymbol{\sigma}$ and $\boldsymbol{\epsilon}$ are homogeneous and given in the cylindrical frame $(r\theta z)$ by :

$$\boldsymbol{\sigma} = \begin{pmatrix} 0 & 0 & 0 \\ 0 & 0 & \tau \\ 0 & \tau & 0 \end{pmatrix} \quad \boldsymbol{\epsilon} = \begin{pmatrix} 0 & 0 & 0 \\ 0 & 0 & \gamma/2 \\ 0 & \gamma/2 & 0 \end{pmatrix} \tag{1}$$

where γ is the distortion (corresponding to twice the shear strain term - see figure 2a). The shear behaviour of a material is obtained by plotting the shear stress τ as function of the distortion γ. τ is linked to the torque C by:

$$\tau = \frac{C(R_o + R_i)}{\pi(R_o^4 - R_i^4)} \tag{2}$$

R_o and R_i are the outer and inner radii of the cylinder. The test specimen has been meticulously sized using a nonlinear mechanical finite element formulation (and a constitutive behaviour obtained from a previous tensile test).

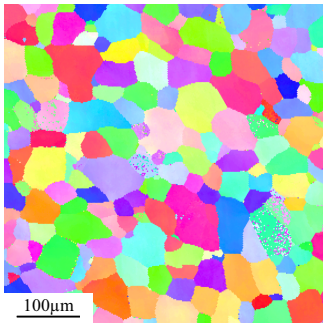

Figure 1: Microstructure of pure iron (ARMCO grade) illustrated by inverse pole figure from electron back-scattered diffraction.

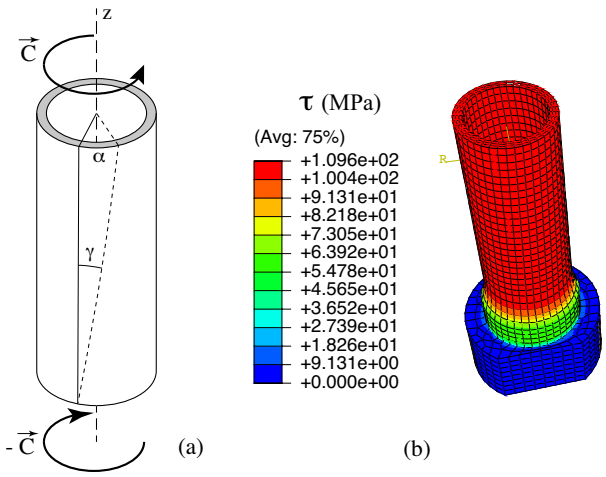

Figure 2: (a) principle of torsion test; (b) optimized (half) geometry and shear stress distribution for C=32Nm.

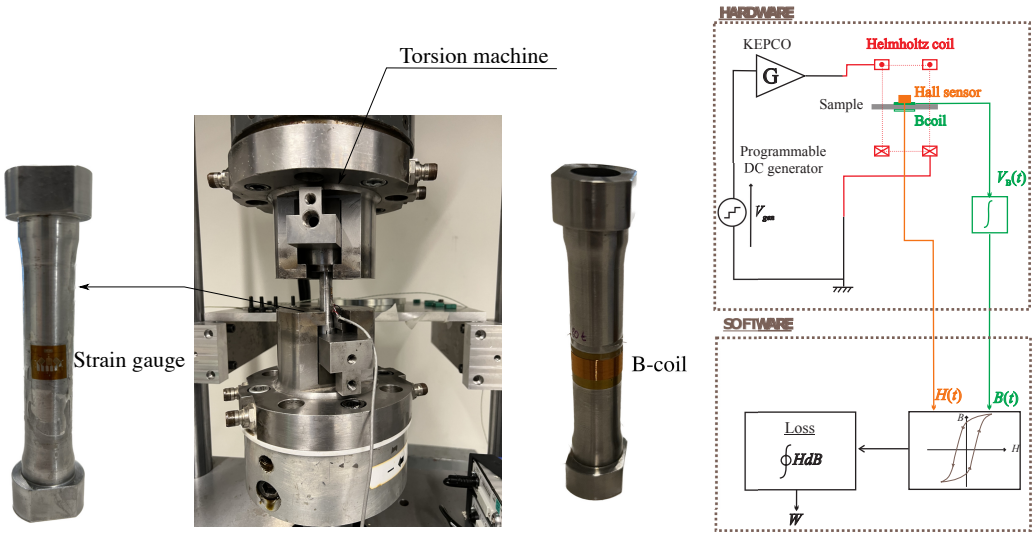

Figure 3: (a) Designed specimen for homogenous shear plasticity ; (b) Testing machine ; (c) specimen after plastic deformation with B-coil; (d) set-up for magnetic measurements

This design has to prevent plastic buckling while ensuring the presence of a sufficiently homogeneous region for accurate magnetic measurements. An illustration of the simulated geometry (half specimen), demonstrating the homogeneity of stress across the specimen, is provided in the figure 2b. It is a dog-bone specimen where heads (in blue) allow for a suitable application of a torque. Inner and outer diameter of final geometry are 13mm and 14.9mm respectively. It defines a homogeneous gauge length of about 71mm. The average fluctuation of the plastic shear strain through the thickness is assessed to be approximately 4%. Mechanical tests were carried out using the MTS hydraulic twisting testing machine with angular control allowing for $\dot{\gamma} = 2 \times 10^{-3} s^{-1}$. Figure 3a and 3b illustrate the specimen and the mechanical setup employed. A strain gauge positioned at 45 degrees from z-axis has been used to measure the local shear strain $\epsilon = \gamma/2$. A measurement error of ± 0.001 on γ can be estimated. As illustrated in figure 3 c), a magnetic measurements set-up based on Helmholtz coils has been used. Indeed, this system allows a homogeneous magnetic field to be applied in the central zone where the sample is placed while providing access to the center of the setup to position a Hall effect sensor for the measurement of the local magnetic field H. The homogeneity of the field in the Hall probe measurement zone has been verified by finite elements calculations. A B-coil wound around the sample in the middle (with a length less than 10 mm) allows for the measurement of the magnetic induction B after analog integration. Power generation is carried out through a programmable generator (used in DC mode), and the power is amplified by a linear amplifier. The measurement principles are given in figure 3 d). A ballistic method [10] has been chosen for the acquisition of the magnetic behaviour removing any dynamic effect since the time delay between each point is large.

3. Results

Specimen #1 is non-deformed and used to get reference magnetic behaviour. Figure 4 reports the shear stress-distortion (τ-γ) curves of the three other deformed specimens. Specimen #2 has been subjected to monotonous torsion up to a plastic distortion (remanent distortion) of about γ_p=+4%. Specimen #3 has been subjected to a cyclic testing beginning by a positive plastic distortion first up to γ_p=+4% then followed by a negative twist reaching a plastic distortion of about -4%. Specimen #4 has been subjected to monotonous high magnitude plastic distortion up to γ_p=12%.

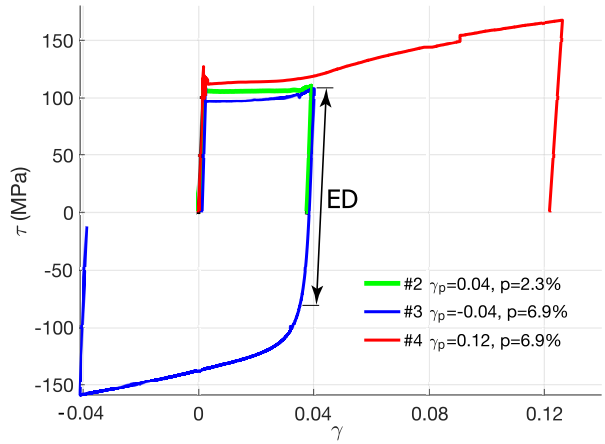

Figure 4: shear stress vs shear strain (τ-γ) history of conducted tests. ED: elastic domain after deformation of specimen #2.

Following Levy-Mises description, the cumulative plastic strain is defined as :

$$p = \int_0^T \sqrt{\frac{2}{3}\dot{\boldsymbol{\epsilon}}_p : \dot{\boldsymbol{\epsilon}}_p}\, dt \tag{3}$$

with $\boldsymbol{\epsilon}_p$ the plastic strain tensor and T the end time of mechanical test. Considering pure plastic shear strain, the cumulative plastic strain writes :

$$p = \int_0^T \left| \frac{\dot{\gamma}_p}{\sqrt{3}} \right| dt \tag{4}$$

This parameter is usually related to the defects quantity. Specimen #3 and #4 are characterized by the same level of cumulative plastic strain but different plastic strain levels (figure 4).

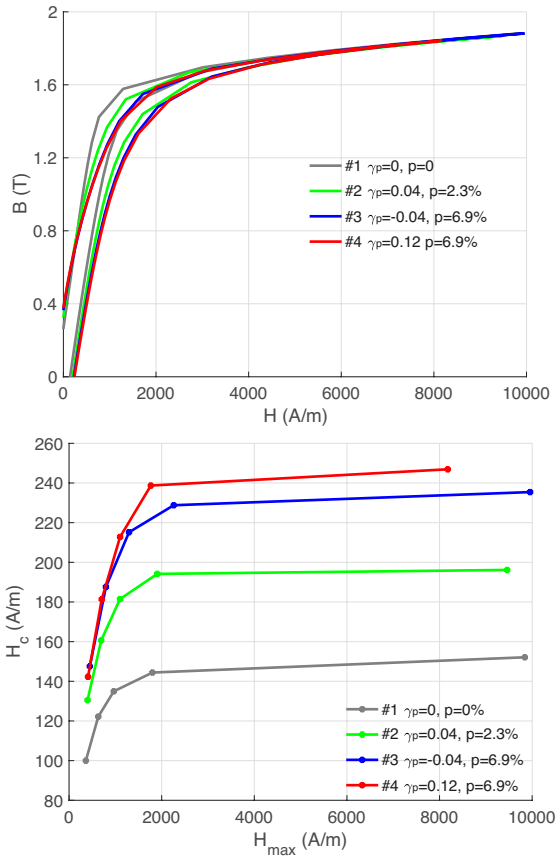

Figure 5: a) Experimental hysteresis cycles for the tested specimens. b) coercive field variation according to maximum magnetic field

Figure 5a shows the experimental major $B(H)$ loops for the tested specimens. The main effects that can be observed relate to the saturation knee region: the undeformed specimen presents the highest induction level. Plasticity leads to a decreasing of magnetic induction consistent with the observations made by many authors. It is remarkable to note that the evolution of the induction is correlated with the level of cumulative plasticity but is not correlated with the plastic strain level: the behavior of specimen #2 is intermediate between that of specimen #1 and #4. Specimen #3 and #4, characterized by a same level of cumulative plastic deformation, exhibit similar magnetic behaviours (specimen #4 is slightly more deformed than specimen #3 as observed in figure 4 explaining the hierarchy), Specimen #2 and #3, which have been subjected to the same absolute level of plastic deformation $|\gamma_p|$, exhibit different behaviours.

Figure 5b shows the variation of coercive field H_c extracted from all magnetic data as a function of maximum magnetic field level H_{max} of various loops. The coercive field increases nonlinearly with respect to the maximum applied magnetic field as expected. It increases too as function of the cumulative plastic strain. Values reached are significantly higher than values for reference specimen. Again, coercive field curves of specimen #3 and #4 are very close to each other. The same conclusion applies when looking at the energy density losses W (area of hysteresis loops) as function of maximal magnetic induction B_{max} in figure 6. Energy losses look however slightly higher for specimen #4 than for specimen #3. This may be explained by small differences of true cumulative plastic strain or other factors discussed in the last section.

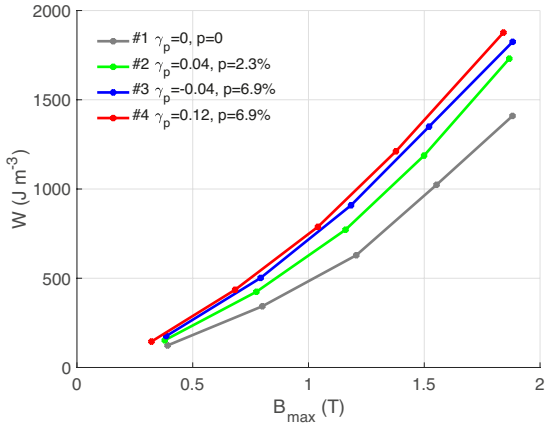

Figure 6: Static magnetic energy density losses for samples #1 to #4

Figures 7a to 7c represent finally maximum relative permeability μ_{mr} (highest average slope of $B(H)$ curves), maximum coercive field (evaluated at H_{max}=8000A/m), magnetic energy density losses (evaluated at B_{max}=1.5T) as function of cumulative plastic strain. Conclusions join the previous comments: cumulative plastic strain seems to be a relevant mechanical term that correlates with the variations of magnetic quantities.

4. Discussion

It can be observed first that results obtained in this study join the stablished knowledge in the literature: plastic strain "degrades" the magnetic behaviour. This study shows that the mode of deformation appears to have minimal or possibly negligible involvement in the process: Shear plastic strain acts qualitatively similarly to tensile plastic strain [6]. This study shows on the other hand that cumulative plastic strain is relevant unlike plastic strain level. It is not possible to observe such effect by a simple tensile testing. Cumulative plastic strain is well known to be related to microstructural defects such as dislocations [11]: indeed accumulation of dislocations serves as pinning sites for magnetic domain walls [12]. That leads several researchers to propose a relationship between coercive field and dislocation density [13].

In some recent works, it has been proposed to link the variation of magnetic behaviour to internal stresses that occur with

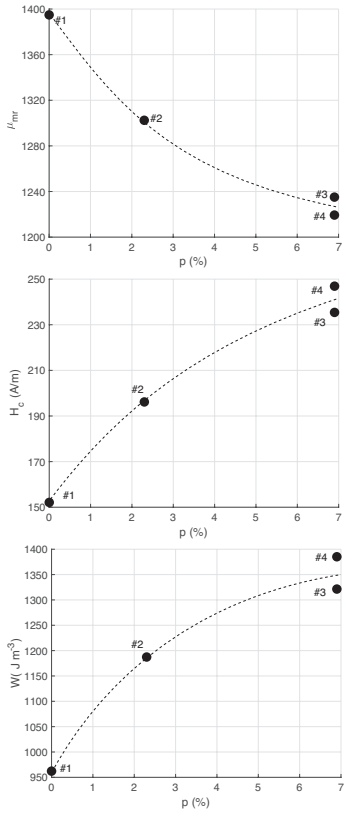

Figure 7: Maximal relative permeability (a), coercive field at H_{max}=8000A/m (b) and static magnetic energy density losses at B=1.5T (c) as function of cumulative plastic strain.

plastic straining [14]. This approach allows for the understanding why a plastic compression can improve the magnetic behaviour of a pipeline steel unlike a plastic tension [15]. Indeed the same cumulative plastic strain can be reached by tension and compression. Since behaviours are different, interpretation using internal stresses may be relevant. Figure 4 shows the experimental $\tau(\gamma)$ results. Experiment with specimen #2 involves a cyclic torsion that allows for an observation of the new elastic domain (ED) after the first loading. This domain is not symmetric with respect to $\tau = 0$ axis, meaning that internal stresses have been developed [16]. Following the proposition of [8], a material can be divided in soft (s) and hard (h) phases (even in a single phase material). Residual stresses in each phase are given by :

$$\boldsymbol{\sigma_s} = -\boldsymbol{X} \quad \text{and} \quad \boldsymbol{\sigma_h} = \frac{f_s}{f_h}\boldsymbol{X} \tag{5}$$

f_s and f_h are the volume fractions of the soft and hard phases and $\boldsymbol{X}$ the macroscopic kinematic hardening tensor. In case of pure shear stress-strain loading, the kinematic hardening tensor follows the plastic strain tensor and writes:

$$\boldsymbol{X} = \begin{pmatrix} 0 & 0 & 0 \\ 0 & 0 & X_{\theta z} \\ 0 & X_{\theta z} & 0 \end{pmatrix} \tag{6}$$

The stress state in each of phase is therefore deviatoric. We then employ the principle of equivalent stress proposed in [17] to assess the effect of this particular residual stress state on the magnetic behaviour. The equivalent stress writes:

$$\sigma_{eq} = \frac{3}{2}\,{}^t\vec{n}.\boldsymbol{\sigma}_D.\vec{n} \tag{7}$$

where $\vec{n}$ indicates the magnetic measurement direction and $\boldsymbol{\sigma}_D$ the stress deviator. Applied to the present situation, $\vec{n}$ is corresponding to direction z, $\boldsymbol{\sigma}_D = \boldsymbol{\sigma_s}$ for the soft phase and $\boldsymbol{\sigma}_D = \boldsymbol{\sigma_h}$ for the hard phase. Calculation shows that the equivalent stress is null for both phases. This means that residual stresses, even existing, have no effect on the magnetic behaviour according to this model. The torsion test therefore has the advantage to allow for an observation of the effect of defects on the magnetic behaviour, without being masked by the effect of internal stresses. This result can explain why specimen #3 and #4 exhibit similar magnetic behaviour despite a probably different residual stress state (since plastic strain level and sign are different).

5. Conclusion

To the best knowledge of authors, it is the first time that effect of plastic shear strain on magnetic behaviour is reported. This work highlights the very significant role of cumulative plastic strain on the magnetic behaviour, leading to a global degradation of magnetic performances of a soft magnetic material: decreasing of permeability; increasing of coercive field and static power losses. On the contrary, the deformation level is not the relevant parameter. The torsion test also leads to a deviatoric residual stress state whose influence is negligible when magnetic measurement is carried out along the torsion axis. The experimental protocol therefore makes it possible to observe the sole influence of defects generated by plasticity on magnetic behavior.

References

[1] V. Shullani, et al. *Sensors*, 17(12):2799, 2017.
[2] Z. Maazaz, et al. *NDT & E Int.*, 134:102782, 2023.
[3] P. Vourna, et al. *NDT & E Int.*, 139:102933, 2023.
[4] F. Wu, et al. *JMMM*, 551:169185, 2022.
[5] S.M. Thompson and B.K. Tanner. *JMMM.*, 83(1):221–222, 1990.
[6] E. Hug, et al. *IEEE Trans. on Magn.*, 33(1):763–771, 1997.
[7] C. C. H. Lo, et al. *J. of Appl. Physics*, 93(10):6626–6628, 05 2003.
[8] O. Hubert and S. Lazreg. *JMMM*, 424:421–442, 2017.
[9] E. Hug. *J. Mat. Sc.*, 30:4417–4424, 1995.
[10] F. Fiorillo *Measurement and characterization of magnetic materials*. ed. North-Holland, 2004, p118.
[11] P.M. Anderson, J.P. Hirth, and J. Lothe. *Theory of dislocations*. 3rd ed. Cambridge University Press, 2017.
[12] H.R. Hilzinger and H. Kronmüller. *JMMM*, 2(1):11–17, 1975.
[13] J. Li, M. Xu, et al. *J. of Appl. Physics*, 111(6):063909, 03 2012.
[14] O.Hubert et al. *J. Phys. IV France*, 08(2):515–518, 1998.
[15] Z. Maazaz, O. de La Barrière, and O. Hubert. Influence of plastic compression on the magnetic behaviour of a pipeline steel. In *Proceedings of the 25th Soft Magnetic Conference (SMM25)*, Grenoble, France, 2021.
[16] D. François, A. Pineau, and A. Zaoui. *Mechanical Behaviour of Materials - Volume I: Elasticity and Plasticity*. Springer, 1998.
[17] O. Hubert and L. Daniel. *JMMM*, 323(13):1766–1781, 2011.